C

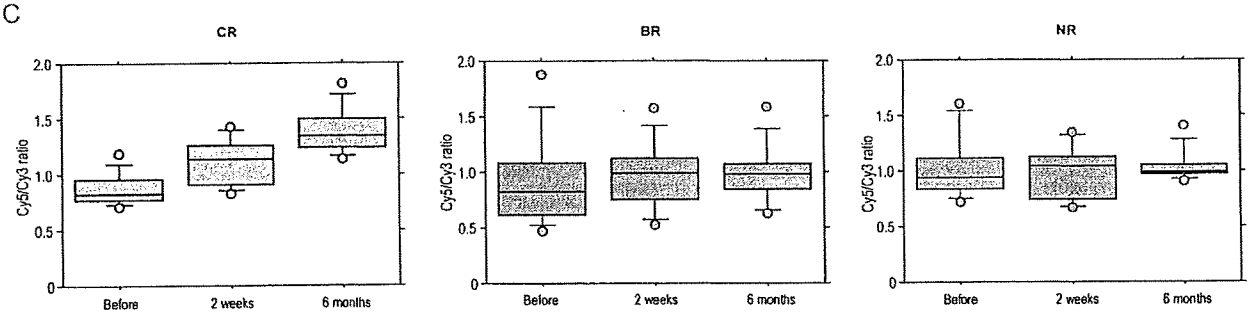

Serine (or cysteine) proteinase inhibitor, clade A*	Bruton agammaglobulinemia tyrosine kinase
Ribosomal protein S27 (metallopanstimulin 1)	*LITAF*
Eukaryotic translation elongation factor 2	Hemopoietic cell kinase
Epidermal growth factor receptor	*GZMA*
Hemopoietic cell kinase	

D

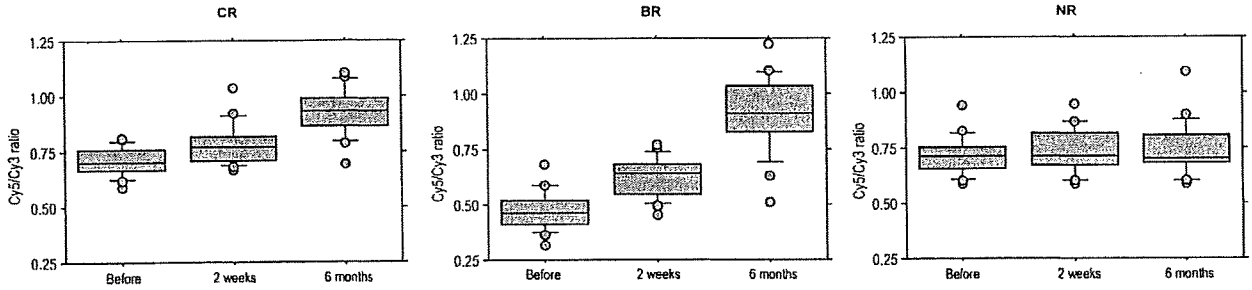

Interleukin 2 receptor beta chain	***ADP-ribosyltransferase****	Semaphorin (CD100)
ICE	Interleukin enhancer binding factor 1	Mitochondrial 2,4-dienoyl-CoA reductase
Ribosomal protein S16	CD3D antigen, delta polypeptid	***Ras-related C3 botulinum toxin substrate 2****
Glutamate dehydrogenase 1	Fc fragment of IgE, low affinity II, receptor	*E2L1*
Small nuclear ribonucleoprotein polypeptide N	Selectin L (lymphocyte adhesion molecule 1)	Citrate synthase
Mutant lymphocyte-specific protein tyrosine kinase	Ikaros/LyF-1 homolog (hlk-1)	*ERP72*

E

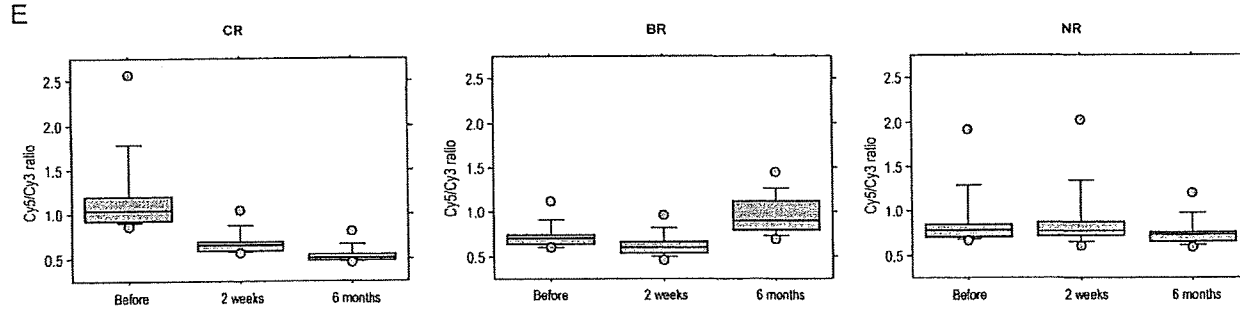

Baculoviral IAP repeat–containing 2*	Rho-associated, coiled-coil containing protein kinase 1
MIHC*	***Apoptosis inhibitor 1****
NRAS-related gene	Uracil-DNA glycosylase
Reticulocalbin 2, EF-hand calcium binding domain	Damage-specific DNA binding protein 1 (127kD)
ERCC5*	CD69 antigen (p60, early T-cell activation antigen)
Integrin, beta 1	

Figure 4. *(Continued.)*

Table 5. Ten gene combinations selected by the SWEEP operator method for the construction of chronic hepatitis C class prediction 2 weeks after the start of interferon (IFN) therapy.

Combination	Input	Gene name	GenBank accession no.	Accuracy, %	
				Training	Test
1	1	*ERCC5*	NM_000123	55.3	45.5
	2	Serine (or cysteine) proteinase inhibitor clade A member 1	NM_000295	85.6	54.5
	3	Ras homolog gene family member A	NM_001664	80.3	70.5
2	1	Baculoviral IAP repeat–containing 2	NM_001166	47.7	41.7
	2	Serine (or cysteine) proteinase inhibitor clade A member 1	NM_000295	80.3	53.8
	3	Ras homolog gene family member A	NM_001664	80.3	70.5
3	1	Cyclin G1	NM_004060	36.6	44.0
	2	Ras-related C3 botulinum toxin substrate 2	NM_002872	79.6	61.4
	3	*EST*		70.5	56.8
4	1	Ecotropic viral integration site 2A	NM_001003927	41.7	25.8
	2	Peptidylprolyl isomerase D (cyclophilin D)	NM_005038	60.6	46.2
	3	Cyclin G1	NM_004060	77.3	67.4
5	1	***Myeloid cell nuclear differentiation antigen***[a]	NM_002432	55.3	25.8
	2	Cyclin G1	NM_004060	85.6	64.4
	3	ADP-ribosyltransferase (NAD+; poly [ADP-ribose] polymerase)	NM_001618	80.3	87.1
6	1	Integrin β1	NM_033666	47.7	19.7
	2	Cyclin G1	NM_004060	80.3	62.9
	3	***STAT1***[a]	NM_139266	80.3	68.2
7	1	Differentiation 6 (septin 2)	NM_004404	28.8	25.8
	2	Cyclin G1	NM_004060	75.0	64.4
	3	Cell division cycle 20 homolog *(S. cerevisiae)*	NM_001255	90.2	87.9
8	1	*MIHC*	NM_001165	28.8	25.0
	2	Cyclin G1	NM_004060	75.0	64.4
	3	Cell division cycle 20 homolog *(S. cerevisiae)*	NM_001255	90.2	87.9
9	1	Apoptosis inhibitor 1 (baculoviral IAP repeat–containing 3)	NM_001165	28.8	25.0
	2	Cyclin G1	NM_004060	75.0	64.4
	3	Cell division cycle 20 homolog *(S. cerevisiae)*	NM_001255	90.2	87.9
10	1	Nuclear factor (erythroid-derived 2)–like 1	NM_003204	25.0	25.8
	2	Cyclin G1	NM_004060	75.0	63.6
	3	ADP-ribosyltransferase (NAD+; poly [ADP-ribose] polymerase)	NM_001618	88.6	81.8

[a] Genes that present similar expression patterns during IFN and ribavirin combination therapy.

CR group, the expression profiles of genes that were either up- or down-regulated before IFN therapy were similar to those of healthy volunteers 6 months after the end of IFN therapy (figure 2*A*, CR group). On the other hand, in the NR group, expression of genes that were either up- or down-regulated before IFN therapy tended to remain up- or down-regulated 6 months after the end of IFN therapy (figure 2*A*, NR group). This suggests that the changes in gene-expression profiles of patients with CH-C before IFN therapy reflect the state of HCV infection.

We performed real-time PCR to corroborate the microarray data. Real-time PCR revealed that *CD69* was up-regulated in patients with CH-C and that *CCR2* and *IL7R* were down-regulated in patients with CH-C (figure 2*B* and table 2).

Relationship between PBMC gene-expression profiles and IFN response. We then analyzed the relationship between PBMC gene-expression profiles before the start of IFN therapy and IFN response. Because the regimen of IFN treatment was different in group A and group B patients, we first focused on group A patients (table 1). In hierarchical clustering analysis using all genes before IFN therapy, no clustering was seen in the CR, BR, or NR groups. Conventional supervised learning methods, such as support vector machine and nearest neighbor (BRB-ArrayTools), could not discriminate between the CR, BR, and NR groups. Therefore, we applied the FNN-SWEEP method to predict the outcome of IFN therapy. Before FNN-

Table 6. Comparison of interferon (IFN)–stimulated gene (ISG) expression induced by IFN.

The table is available in its entirety in the online edition of the *Journal of Infectious Diseases*.

SWEEP analysis, nonspecific genes or genes with errors were eliminated by the PART method. The 32 genes screened by PART are shown in figure 3. Topoisomerase (DNA) I *(TOP1)* and interleukin 2 receptor β *(IL2RB)* were up-regulated in the CR group, hemoglobin γG *(HBG2)* and monocyte chemotactic protein were up-regulated in the BR group, and chemokine (C-C motif) ligand 4 and ras-related C3 botulinum toxin substrate 2 *(RAC2)* were up-regulated in the NR group. Genes selected by PART were subjected to the FNN-SWEEP method to construct a class prediction model. Consequently, we selected 10 gene combinations by the SWEEP operator method for CH-C class prediction before the start of IFN therapy (table 4). The most effective gene combination for the prediction of an IFN response was *TOP1;* catenin (cadherin-associated protein) β1 (88 kDa); and *RAC2*. The accuracy of the training and test sets were high, at 91.0% and 89.1%, respectively.

Changes in gene-expression profiles over the course of IFN therapy. We next focused on the changes in gene-expression profiles over the course of IFN therapy and their relationship with IFN response. Using PART, 86 genes with changes in expression between before and 2 weeks after the start of IFN therapy were selected. To investigate the relationship between the 86 genes with changes due to IFN therapy and the efficacy of IFN therapy, changes in the expression of the 86 genes were determined for the CR group. On the basis of self-organizing maps, changes in gene expression in the CR group were classified into the following 5 patterns (figure 4): pattern A, up-regulated 2 weeks after the start of IFN therapy and then down-regulated after the end of IFN therapy; pattern B, down-regulated 2 weeks after the start of IFN therapy and then up-regulated after the end of IFN therapy; pattern C, up-regulated 2 weeks after the start of IFN therapy and also up-regulated after the end of IFN therapy; pattern D, up-regulated at 2 weeks after the start of IFN therapy and then returned to normal after the end of IFN therapy; and pattern E, down-regulated at 2 weeks after the start of IFN therapy and also down-regulated after the end of IFN therapy. Patterns A and B represent gene groups with temporary changes during IFN therapy, whereas patterns C, D, and E represent gene groups with changes after the end of IFN therapy and are thought to be attributable to viral eradication or normalization of hepatic function. Interestingly, very little change was seen in the patterns for the NR group. Therefore, changes in gene expression are also useful in predicting therapeutic efficacy. From the 86 genes isolated by PART, the SWEEP operator method was used to identify 10 gene combinations, and therapeutic efficacy was predicted according to the FNN-SWEEP method (table 5). The results showed that the accuracy for gene combinations 7, 8, and 9 was high, at 90.2%. LOOCV confirmed the high accuracy (87.9%) of prediction using these gene combinations. These combinations included the following genes that are important for predicting therapeutic efficacy: *CDC20* was classified as belonging to pattern A; cyclin G1 and differentiation 6 were as belonging to pattern B; and *MIHC* and apoptosis inhibitor 1 were as belonging to pattern E (figure 4).

IFN and ribavirin combination therapy. We then investigated the usefulness of the above-mentioned genes in predicting the efficacy of IFN and ribavirin combination therapy. It has been shown that concurrent ribavirin administration improves the rate of CR. In addition, the changes in gene expression during combination therapy are due not only to IFN but also to ribavirin. Thus, the results for monotherapy may not be applicable to combination therapy. However, changes in the expression of several genes—CD2 antigen (p50), *IL2RB, HBG2,* myeloid cell nuclear differentiation antigen *(MNDA),* and *STAT1*—were shown to be extremely useful for distinguishing CR from NR in IFN and ribavirin combination therapy (tables 4 and 5).

DISCUSSION

HCV load, genotype, and fibrosis have been listed as factors that influence the effectiveness of IFN therapy [4, 5], but these factors are not sufficient, and other predictive factors are needed. Unlike liver-biopsy specimens, PBMCs can be easily collected, and collection can be repeated as necessary. We analyzed the gene-expression profiles of PBMCs in patients with CH-C by use of cDNA microarrays under the hypothesis that gene expression in PBMCs is indicative of IFN efficacy and CH-C disease state. In addition, changes in the gene-expression profiles of PBMCs were analyzed during the course of IFN therapy to clarify the relationship between gene-expression profiles of PBMCs and IFN response.

Interestingly, the gene-expression profiles of PBMCs from patients with CH-C and from healthy volunteers were different, and this was confirmed by hierarchical clustering analysis and supervised learning analysis using support vector machine. When patients with CH-C and healthy volunteers were compared, gene expression in the JAK-STAT cascade, humoral immune response, and G protein–coupled receptor protein signaling pathway differed markedly. In most patients with CH-C, expression of these genes is activated, and HCV infection is thought to bring about changes in the gene expression in PBMCs. Several chemokine- and cytokine-related genes, such as *CCR2* and *IL7R,* were down-regulated. Although the reason for this was not clear, expression of these genes in liver-infiltrating lymphocytes was up-regulated. Therefore, the down-regulation of immune-related genes may represent increased levels of liver-infiltrating lymphocytes accompanying hepatitis. Interestingly, when the chronological changes in PBMC gene-expression profiles were analyzed for the CR group, the profiles at 6 months after the end of therapy were similar to those of healthy volunteers. Therefore, the changes in gene-expression

profiles before IFN therapy were due to HCV infection. On the other hand, the gene-expression profiles of the NR group before IFN therapy were similar to those at 6 months after the end of IFN therapy (figure 2*A*).

Unfortunately, it was not possible to differentiate between CR, BR, and NR patients on the basis of gene-expression profiles of PBMCs by use of nonsupervised learning methods, such as hierarchical clustering, before IFN therapy. Therefore, we used FNN theory for CH-C class prediction. The most attractive feature of FNN is that causality between input and output variables can be described very accurately as explicit if-then roles obtained from the constructed model. For the purpose of analyzing numerous genes in a short time, FNN combined with the SWEEP operator method was developed (FNN-SWEEP method) and has been shown to be a precise, simple tool for predicting patient survival on the basis of microarray data [28, 29]. In addition, by first filtering genes by use of PART, the accuracy of the FNN-SWEEP method was further increased [30]. In the present study, a total of 32 genes were identified by PART on the basis of genetic changes before therapy, and, in the CR group, expression of genes such as *TOP1*, *IL2RB*, prothymosin α *(PTMA)*, and ADP-ribosyltransferase was up-regulated, thus indicating active cellular proliferation. In the NR group, the expression of genes indicating activated cytotoxic T cells—such as granzyme, CD2 antigen, *RAC2*, and natural killer cell transcript 4—was up-regulated. Because these genes were up-regulated by IFN therapy in the CR group, they were thought to be up-regulated before therapy in the NR group. Lempicki et al. reported elevated expression of endogenous IFN/innate immune response genes in PBMCs from NR patients coinfected with HCV and HIV [31]. This suggests that, in many NR patients, few immune effector cells are active or that these effector cells cannot infiltrate the liver and remain in the peripheral blood.

To further investigate the above-mentioned points, changes in the gene-expression profiles of PBMCs were determined during the course of IFN therapy. On the basis of expression profiles before and 2 weeks after the start of IFN therapy, 86 genes were selected. These genes did not include as many IFN-α–stimulated genes as were noted in liver [25–27] (table 6), but they included valuable immune regulatory genes.

On the basis of self-organizing maps, changes in gene expression in the CR group were then classified into 5 patterns (figure 4). These gene groups represent genes with temporary changes due to IFN therapy and those with changes after the end of IFN therapy. Gene groups with changes after the end of IFN therapy are thought to be involved in viral eradication or the normalization of hepatic function. Interestingly, little change was seen in any of the patterns in the NR group. In efficacy prediction by the FNN-SWEEP method, the accuracy for the gene combinations 7, 8, and 9 was high, at 90.2%, thus suggesting that changes in gene expression 2 weeks after the start of IFN therapy are also useful in predicting therapeutic efficacy.

We also investigated whether these genes are useful in predicting the efficacy of IFN and ribavirin combination therapy. Changes in gene expression during combination therapy were due not only to IFN but also to ribavirin, and the results for monotherapy could not simply be applied to combination therapy. However, changes in the expression of several genes—CD2 antigen (p50), *IL2RB*, *HBG2*, *MNDA*, and *STAT1*—were shown to be extremely useful for distinguishing CR from NR in IFN and ribavirin combination therapy.

Unfortunately, because the number of subjects in the present study was small, the genes that were identified as predictors for IFN monotherapy were not necessarily predictors for IFN and ribavirin combination therapy. However, the present study was the first to show that responses to IFN therapy could be predicted on the basis of changes in gene expression by PBMCs, and further investigations in greater numbers of patients are required.

Acknowledgments

We thank Prof. Kenichi Kobayashi, for helpful discussion and advice. We also thank A. Nakano, M. Ueda, and J. Hara, for their valuable technical assistance.

References

1. McHutchison JG, Gordon SC, Schiff ER, et al. Interferon alfa-2b alone or in combination with ribavirin as initial treatment for chronic hepatitis C. Hepatitis Interventional Therapy Group. N Engl J Med 1998; 339:1485–92.
2. Davis GL, Esteban-Mur R, Rustgi V, et al. Interferon alfa-2b alone or in combination with ribavirin for the treatment of relapse of chronic hepatitis C. International Hepatitis Interventional Therapy Group. N Engl J Med 1998; 339:1493–99.
3. Poynard T, Marcellin P, Lee SS, et al. Randomised trial of interferon alpha2b plus ribavirin for 48 weeks or for 24 weeks versus interferon alpha2b plus placebo for 48 weeks for treatment of chronic infection with hepatitis C virus. International Hepatitis Interventional Therapy Group. Lancet 1998; 352:1426–32.
4. Martinot-Peignoux M, Marcellin P, Pouteau M, et al. Pretreatment serum hepatitis C virus RNA levels and hepatitis C virus genotype are the main and independent prognostic factors of sustained response to interferon alfa therapy in chronic hepatitis C. Hepatology 1995; 22: 1050–6.
5. Tsubota A, Chayama K, Ikeda K, et al. Factors predictive of response to interferon-alpha therapy in hepatitis C virus infection. Hepatology 1994; 19:1088–94.
6. Mizukoshi E, Kaneko S, Yanagi M, et al. Expression of interferon alpha/beta receptor in the liver of chronic hepatitis C patients. J Med Virol 1998; 56:217–23.
7. Ortaldo JR, Mantovani A, Hobbs D, Rubinstein M, Pestka S, Herberman RB. Effects of several species of human leukocyte interferon on cytotoxic activity of NK cells and monocytes. Int J Cancer 1983; 31: 285–9.
8. Tsubouchi E, Akbar SM, Horiike N, Onji M. Infection and dysfunction

of circulating blood dendritic cells and their subsets in chronic hepatitis C virus infection. J Gastroenterol 2004; 39:754–62.
9. Popov S, Chenine AL, Gruber A, Li PL, Ruprecht RM. Long-term productive human immunodeficiency virus infection of CD1a-sorted myeloid dendritic cells. J Virol 2005; 79:602–8.
10. Schena M, Shalon D, Davis RW, Brown PO. Quantitative monitoring of gene expression patterns with a complementary DNA microarray. Science 1995; 270:467–70.
11. Schena M, Shalon D, Heller R, Chai A, Brown PO, Davis RW. Parallel human genome analysis: microarray-based expression monitoring of 1000 genes. Proc Natl Acad Sci USA 1996; 93:10614–9.
12. DeRisi J, Penland L, Brown PO, et al. Use of a cDNA microarray to analyse gene expression patterns in human cancer. Nat Genet 1996; 14:457–60.
13. Khan J, Simon R, Bittner M, et al. Gene expression profiling of alveolar rhabdomyosarcoma with cDNA microarrays. Cancer Res 1998; 58: 5009–13.
14. Iyer VR, Eisen MB, Ross DT, et al. The transcriptional program in the response of human fibroblasts to serum. Science 1999; 283:83–7.
15. Heller RA, Schena M, Chai A, et al. Discovery and analysis of inflammatory disease-related genes using cDNA microarrays. Proc Natl Acad Sci USA 1997; 94:2150–5.
16. Alizadeh AA, Eisen MB, Davis RE, et al. Distinct types of diffuse large B-cell lymphoma identified by gene expression profiling. Nature 2000; 403:503–11.
17. Desmet VJ, Gerber M, Hoofnagle JH, Manns M, Scheuer PJ. Classification of chronic hepatitis: diagnosis, grading and staging. Hepatology 1994; 19:1513–20.
18. Tanaka T, Tsukiyama-Kohara K, Yamaguchi K, et al. Significance of specific antibody assay for genotyping of hepatitis C virus. Hepatology 1994; 19:1347–53.
19. Kawai HF, Kaneko S, Honda M, Shirota Y, Kobayashi K. Alpha-fetoprotein-producing hepatoma cell lines share common expression profiles of genes in various categories demonstrated by cDNA microarray analysis. Hepatology 2001; 33:676–91.
20. Honda M, Kaneko S, Kawai H, Shirota Y, Kobayashi K. Differential gene expression between chronic hepatitis B and C hepatic lesion. Gastroenterology 2001; 120:955–66.
21. Shirota Y, Kaneko S, Honda M, Kawai HF, Kobayashi K. Identification of differentially expressed genes in hepatocellular carcinoma with cDNA microarrays. Hepatology 2001; 33:832–40.
22. Honda M, Shimazaki T, Kaneko S. La protein is a potent regulator of replication of hepatitis C virus in patients with chronic hepatitis C through internal ribosomal entry site-directed translation. Gastroenterology 2005; 128:449–62.
23. Kawaguchi K, Honda M, Yamashita T, Shirota Y, Kaneko S. Differential gene alteration among hepatoma cell lines demonstrated by cDNA microarray-based comparative genomic hybridization. Biochem Biophys Res Commun 2005; 329:370–80.
24. Honda M, Kawai H, Shirota Y, Yamashita T, Kaneko S. Differential gene expression profiles in stage I primary biliary cirrhosis. Am J Gastroenterol 2005; 100:2019–30.
25. Honda M, Yamashita T, Ueda T, Takatori H, Nishino R, Kaneko S. Different signaling pathways in the livers of patients with chronic hepatitis B or chronic hepatitis C. Hepatology 2006; 44:1122–38.
26. Smith MW, Walters KA, Korth MJ, et al. Gene expression patterns that correlate with hepatitis C and early progression to fibrosis in liver transplant recipients. Gastroenterology 2006; 130:179–87.
27. Bigger CB, Guerra B, Brasky KM, et al. Intrahepatic gene expression during chronic hepatitis C virus infection in chimpanzees. J Virol 2004; 78:13779–92.
28. Ando T, Suguro M, Kobayashi T, Seto M, Honda H. Selection of casual gene sets for lymphoma prognostication from expression profiling and construction of prognostic fuzzy neural network models. J Biosci Bioeng 2003; 96:161–7.
29. Ando T, Suguro M, Kobayashi T, Seto M, Honda H. Multiple fuzzy neural network system for outcome prediction and classification of 220 lymphoma patients on the basis of molecular profiling. Cancer Sci 2003; 94:906–13.
30. Takahashi H, Kobayashi T, Honda H. Construction of robust prognostic predictors by using projective adaptive resonance theory as a gene filtering method. Bioinformatics 2005; 21:179–86.
31. Lempicki RA, Polis MA, Yang J, et al. Gene expression profiles in hepatitis C virus (HCV) and HIV coinfection: class prediction analyses before treatment predict the outcome of anti-HCV therapy among HIV-coinfected persons. J Infect Dis 2006; 193:1172–7.

Cancer Immunol Immunother
DOI 10.1007/s00262-009-0796-2

ORIGINAL ARTICLE

EphA2-derived peptide vaccine with amphiphilic poly(γ-glutamic acid) nanoparticles elicits an anti-tumor effect against mouse liver tumor

Shinjiro Yamaguchi · Tomohide Tatsumi · Tetsuo Takehara · Akira Sasakawa · Masashi Yamamoto · Keisuke Kohga · Takuya Miyagi · Tatsuya Kanto · Naoki Hiramastu · Takami Akagi · Mitsuru Akashi · Norio Hayashi

Received: 21 August 2009 / Accepted: 10 November 2009

Abstract The prognosis of liver cancer remains poor, but recent advances in nanotechnology offer promising possibilities for cancer treatment. Novel adjuvant, amphiphilic nanoparticles (NPs) composed of L-phenylalanine (Phe)-conjugated poly(γ-glutamic acid) (γ-PGA-Phe NPs) having excellent capacity for carrying peptides, were found to have the potential for use as a peptide vaccine against tumor models overexpressing artificial antigens, such as ovalbumin (OVA). However, the anti-tumor potential of γ-PGA-Phe NPs vaccines using much less immunogenic tumor-associated antigen (TAA)-derived peptide needs to be clarified. In this study, we evaluated the effectiveness of immunization with EphA2, recently identified TAA, derived peptide-immobilized γ-PGA-Phe NPs (Eph-NPs) against mouse liver tumor of MC38 cells (EphA2-positive colon cancer cells). Immunization of normal mice with Eph-NPs resulted in generation of EphA2-specific type-1 CD8+ T cells. Immunization with Eph-NPs tended to provide a degree of anti-MC38 liver tumor protection more than that observed for immunization with the mixture of EphA2-derived peptide and complete Freund's adjuvant (Eph + CFA). Neither Eph-NPs nor Eph + CFA vaccines inhibited tumor growth of BL6, EphA2-negative melanoma cells. Splenocytes isolated from MC38-bearing mice treated with Eph-NPs showed strong and specific cytotoxic activity against MC38 cells. Immunization with Eph + CFA induced liver damage as evidenced by elevation of serum alanine aminotransferase, while Eph-NPs vaccination did not exhibit any toxic damage to the liver. These results demonstrated that immunization with Eph-NPs displayed anti-tumor effects against liver tumor by generating acquired immunity equivalent to the toxic adjuvant CFA, suggesting that safe γ-PGA-Phe NPs could be applied clinically for the vaccine treatment of liver cancer.

Keywords Peptide vaccine · EphA2-derived peptide · Acquired immunity · Liver tumor

Abbreviations

IFA	Incomplete Freund's adjuvant
NPs	Nanoparticles
γ-PGA	Poly(γ-glutamic acid)
Phe	L-Phenylalanine
CFA	Complete Freund's adjuvant
PBS	Phosphate buffered saline
i.p.	Intraperitoneal
ALT	Alanine aminotransferase
DCs	Dendritic cells

Introduction

Immunotherapies using peptide vaccine combined with immunologic adjuvants, such as incomplete Freund's

S. Yamaguchi and T. Tatsumi contributed equally to this work.

S. Yamaguchi · T. Tatsumi (✉) · T. Takehara · A. Sasakawa · M. Yamamoto · K. Kohga · T. Miyagi · T. Kanto · N. Hiramastu · N. Hayashi
Department of Gastroenterology and Hepatology, Osaka University Graduate School of Medicine, 2-2 Yamadaoka, Suita, Osaka 565-0871, Japan
e-mail: tatsumit@gh.med.osaka-u.ac.jp

T. Akagi · M. Akashi
Department of Applied Chemistry, Graduate School of Engineering, Osaka University, Suita, Japan

S. Yamaguchi · T. Tatsumi · T. Takehara · A. Sasakawa · M. Yamamoto · T. Akagi · M. Akashi · N. Hayashi
Core Research for Evolutional Science and Technology (CREST), Japan Science and Technology Agency (JST), Tokyo, Japan

Published online: 27 November 2009

adjuvant (IFA), saponin QS-21, and several cytokines, could enhance the anti-tumor immune response after immunization [1, 2]. To date, these therapies have been clinically applied to patients with several types of cancer and have shown limited anti-tumor effects [3–7]. This is because dose-limiting toxicities of the adjuvant were often observed or the adjuvant effects of the peptide vaccine were too weak to induce a sufficient anti-tumor effect. At present, only aluminum salt has been approved as an immunological adjuvant for clinical use; it appears to have weak activity as an adjuvant [8]. Thus, a new strategy using strong and safe immunologic adjuvant is needed to improve their clinical efficacy in cancer treatment. Recently, advances in nanotechnology have offered promise for application in medical science. Some investigators have reported testing various kinds of nanoparticles (NPs) using efficient antigen-carriers for their biological potential [9–11]. We previously demonstrated the efficacy of immunotherapies using HIV-capturing non-biodegradable polystyrene NPs in an animal model [12–15]. However, non-biodegradable polystyrene NPs would not be applicable in clinical situations as vaccine material due to their safety issues. To improve NP-based vaccines, we have successfully generated biodegradable NPs composed of poly(γ-glutamic acid) (γ-PGA) and hydrophobic amino acid, L-phenylalanine (Phe) [16]. γ-PGA is a naturally occurring poly(amino acid) that is synthesized by certain strains of *Bacillus*. The polymer is made of D- and L-glutamic acid units linked through the α-amino and the γ-carboxylic acid groups, respectively. γ-PGA is water soluble, biodegradable and edible. Therefore, the potential applications of γ-PGA and its derivatives have been of interest in a broad range of fields, including the medical field [17–19]. γ-PGA-Phe NPs can be degraded by γ-glutamyl transpeptidase [20], which is widely distributed in the entire body, and various molecules such as proteins and peptides can be immobilized on the surface or encapsulated into γ-PGA-Phe NPs [21]. We demonstrated that γ-PGA-Phe NPs have an excellent capacity for carrying various proteins and peptides into antigen-presenting cells such as dendritic cells (DCs) and macrophages [22]. However, previous reports were studies that examined the potential of vaccines with γ-PGA-Phe NPs using artificial antigens, such as OVA, which are much more immunogenic than tumor-associated self-antigens. The anti-tumor potential of tumor-associated antigen (TAA)-derived peptide vaccine must be examined in order to establish peptide vaccine therapy using γ-PGA-Phe NPs.

The liver is the most common site of distal metastasis for tumors developing in distal organs, such as the colon, stomach and pancreas, and the physiological status of this organ correlates with the survival of patients with advanced disease, even if the primary tumor site has been resected curatively [23, 24]. We demonstrated that the recently identified TAA EphA2 is overexpressed in colon cancer tissues and that EphA2-derived peptide pulsed DCs showed the high potential as a cancer vaccine in a mouse tumor model [25, 26], suggesting that EphA2-derived peptide could be applicable to evaluate the potential of peptide vaccines with γ-PGA-Phe NPs.

In the present study, we demonstrated that immunization with EphA2-derived peptide-immobilized γ-PGA-Phe nanoparticles (Eph-NPs) displayed anti-tumor effects against EphA2-expressing liver tumor by eliciting EphA2 antigen-specific acquired immunity equivalent to peptide vaccine using the strongest but very toxic adjuvant, complete Freund's adjuvant (CFA). These results indicate that peptide vaccine using γ-PGA-Phe NPs could be a promising candidate for a vaccine adjuvant against liver cancer.

Materials and methods

Mice

Female C57BL/6 mice were purchased from Clea Japan Inc. (Tokyo, Japan) and were used at 6–8 weeks of age. They were housed under conditions of controlled temperature and light with free access to food and water at the Institute of Experimental Animal Science, Osaka University Graduate School of Medicine. All animals received humane care and our study protocol complied with the institution's guidelines.

Cell lines

MC38 as EphA2-positive cell, a mouse colon carcinoma cell derived from C57BL6/J mice, was generously provided by Dr. Kazumasa Hiroishi (Showa University School of Medicine, Tokyo) [25]. BL6 as EphA2 negative cell, a melanoma cell line, and YAC-1, a sensitive cell line to NK cells were purchased from American Type Culture Collection (Rockville, MD) [25]. These cell lines were maintained in Complete Medium (RPMI medium supplemented with 10% fetal bovine serum, 100 U/ml penicillin and 100 μg/ml streptomycin) at 37°C in 5% CO_2.

Preparation of peptide-immobilized γ-PGA-Phe NPs

Nanoparticles composed of γ-PGA-Phe were prepared as previously described [27]. To prepare EphA2-derived peptide-immobilized NPs (Eph-NPs), a carboxyl group of the γ-PGA-Phe NPs (10 mg/ml) was first activated by water-soluble carbodiimide (1 mg/ml in 20 mM phosphate buffer, pH 5.8) for 20 min. The NPs (5 mg) obtained by centrifugation were mixed with 1 ml EphA2-derived peptide (0.5 mg/ml) in phosphate buffered saline (PBS)

and the mixture was incubated at 4°C for 24 h. After the reaction, the centrifuged NPs were washed three times with PBS and resuspended at 10 mg/ml in PBS. Eph-NPs immobilizing 20 μg of EphA2-derived peptide per 1 mg of NPs were prepared. The particle size distribution and the surface charge of NPs were measured by a dynamic light scattering (DLS) and zeta potential measurement using a Zetasizer Nano ZS (Malvern Instruments, UK). The mean diameters of NPs and Eph-NPs were 219 ± 78 and 246 ± 88 nm (mean ± SD), respectively. The NPs and Eph-NPs had a strongly negative zeta potential (−20 to −25 mV) in PBS.

IFN-γ ELISPOT assays for peptide-reactive CD8+ T cells responses

Splenocytes were harvested 5 days after intraperitoneal (i.p.) immunization of normal mice with various amounts of Eph-NPs or equal amounts of EphA2-derived peptide alone twice with a 1-week interval. In another experiments, splenocytes were harvested 5 days after i.p. immunization of normal mice with 10 μg of Eph-NPs or a mixture of 10 μg of EphA2-derived peptide with CFA (Eph + CFA), 10 μg of Eph peptide only (Eph), the γ-PGA-Phe NPs only (NPs) or PBS twice with a 1-week interval. CD8+ T cells were selectively isolated from splenocytes by magnetic cell sorting using CD8 MicroBeads (Miltenyi Biotec, Gladbach, Germany). Mouse IFN-γ ELISPOT assays were performed using a mouse IFN-γ ELISPOT kit (R&D Systems Inc., Minneapolis, MN) according to the manufacturer's instructions. IFN-γ-secreting cells appeared as blue spots. The data are represented as mean IFN-γ spots ± standard deviation (SD) per 100,000 CD8+ T cells analyzed.

Animal experiments

C57BL/6 mice were immunized intraperioneally with Eph-NPs, Eph + CFA, Eph, NPs or PBS twice a week as above. On day 0, at the time of the second injection with these vaccines, mice were lightly anesthetized by isoflurane and 1×10^6 MC38 cells (EphA2-positive) or 1×10^6 BL6 cells (EphA2-negative) were injected under the capsule of the left medial liver lobe by using a 30-gauge needle as previously described [26]. To prevent leakage, a cotton swab was held over the injection site for 2 min. Skin and peritoneum were closed in a single layer using a nylon suture. The procedure was well tolerated by all animals and no intraoperative or anesthesia-related deaths occurred. Mice were killed 14 days after tumor inoculation and the liver weight was measured. Data are reported as the average liver weights ± SD. All the protocols of animal experiments were approved by Institutional Animal Care and Use Committees of Osaka University Graduate School of Medicine.

Cytolytic assays

Splenocytes were harvested 14 days after tumor inoculation. After 5 days of in vitro stimulation with mitomycin C(MMC) (Kyowa Hakko, Tokyo, Japan)-treated MC38 cells, lymphocytes were analyzed for their ability to kill MC38 tumor cells in 4-h ^{51}Cr release assays as previously described [28]. In some experiments, liver lymphocytes were isolated 1 day after immunization of Eph-NPs into MC38-bearing mice as previously described [26], and subjected to 4-hr ^{51}Cr release assays against NK-sensitive YAC-1 target cells.

In vivo depletion of immune cells

The procedure used in this study was described previously [25]. The efficiency of specific subset depletions (CD4+, CD8+ T cell or NK cell) was confirmed by flow cytometric analysis. In all cases, 99% of the targeted cell subset was specifically depleted (data not shown).

Blood biochemistry test

Blood samples were obtained 7 days after final immunization. Levels of serum alanine aminotransferase (ALT), total bilirubin (TBil), albumin (Alb), and creatinine (Crnn) were measured with a standard UV method using a Hitachi type 7170 automatic analyzer (Tokyo, Japan).

Statistical analyses

Statistical differences between the groups were determined by applying Student's t test with Welch correction or one-way ANOVA after each group had been tested with equal variance and Fisher's exact probability tests. Statistical significance was defined as $P < 0.05$.

Results

Detection of EphA2-derived peptide-specific CD8+ T cells after immunization with Eph-NPs into normal mice

We performed IFN-γ ELISPOT assays to examine whether i.p. injection of Eph-NPs into normal mice could generate CD8+ T cells specific for EphA2-derived peptide. As shown in Fig. 1a, the frequencies of EphA2-derived peptide-specific CD8+ T cells in mice treated with the NPs immobilized with 10 or 50 μg of EphA2-derived peptides were significantly higher than those observed for mice

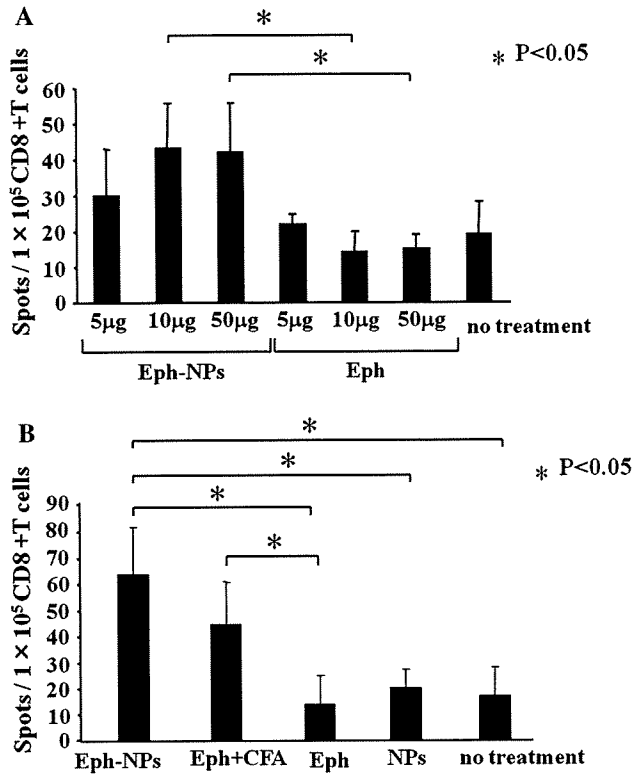

Fig. 1 IFN-γ ELISPOT assays for peptide-reactive CD8+ T cells responses. Normal mice ($N = 3$) were immunized with the indicated dose of Eph-NPs, Eph + CFA, Eph peptide only (*Eph*) or NPs only (*NPs*), and killed on day 5 post-immunization. Spleen cells were harvested and CD8+ T cells isolated using CD8 MicroBeads as described in "Materials and methods". CD8+ T cells were then subjected to IFN-γ ELISPOT assays to detect EphA2-derived peptide-specific CTLs. The data are represented as mean IFN-γ spots ± SD per 100,000 CD8+ T cells analyzed. Similar results were obtained in three independent experiments. $*P < 0.05$

treated with equal amounts of peptides alone. The frequency of EphA2-derived peptide-specific cytotoxic T lymphocytes (CTLs) from mice immunized with the NPs immobilized with 10 μg of EphA2-derived peptides was equal to that from mice treated with NPs immobilized with 50 μg of EphA2-derived peptides. Thus, we used NPs immobilized with 10 μg of EphA2-derived peptides as Eph-NPs vaccines in the following experiments. As shown in Fig. 1b, the frequency of EphA2-derived peptide-specific CD8+ T cells in mice treated with the NPs immobilized with 10 μg of EphA2-derived peptides (Eph-NPs) was significantly higher than that observed for mice treated with NPs alone or EphA2-derived peptides alone. The frequency of EphA2-derived peptide-specific CTLs from mice immunized with Eph-NPs was equal to that from mice treated with mixture of 10 μg of EphA2-derived peptide with CFA (Eph + CFA). These results demonstrated that EphA2-specific type-1 CD8+ T cells (i.e. Tc1) are effectively generated by in vivo immunization with Eph-NPs.

Immunization with Eph-NPs prevents progression of EphA2-expressing liver tumors

We examined whether immunization with the Eph-NPs would promote protective anti-tumor effects against the EphA2-positive MC38 or EphA2-negative BL6 liver tumors. C57BL/6 mice were immunized on day −7 and 0 with Eph-NPs, Eph + CFA, EphA2-derived peptide only (Eph), NPs only (NPs) or PBS. On day 0, at the time of the second injection with these vaccines, mice were lightly anesthetized by isoflurane and 1×10^6 MC38 cells or 1×10^6 BL6 cells were injected under the capsule of the left medial liver lobe. Mice were killed 14 days after tumor inoculation and the liver weight was measured. As shown in Fig. 2a, the liver tumor from mice treated by Eph-NPs tended to be smaller than those from mice treated by Eph + CFA, Eph, NPs or PBS. The liver weights bearing MC38 tumor in mice immunized with Eph-NPs were significantly lighter than those in mice treated with Eph, NPs or PBS. In contrast, those in mice treated with Eph + CFA were not significantly lighter than those in control mice. The liver weights bearing MC38 tumor in mice treated with Eph-NPs tended to be lighter, but not significantly, than those with Eph + CFA (Fig. 2a). Neither Eph-NPs nor Eph + CFA inhibited BL6, EphA2 negative melanoma, tumor growth (Fig. 2b). These results suggest that immunization with Eph-NPs provides specific anti-tumor effects against EphA2-positive MC38 tumors. We also examined the liver weights of mice treated with Eph-NP, Eph + CFA, Eph, NPs or PBS without tumor injection. Mice were treated twice a week with each treatment without tumor injection and evaluated the liver weights 14 days after treatment. The liver weights from all treated mice without tumor injection were almost similar (data not shown), suggesting that each treatment did not affect the liver weight.

Induction of specific CTLs against MC38 cells after immunization with Eph-NPs into MC38 bearing mice

We examined whether immunization of Eph-NPs would induce tumor-specific cytolytic activity against MC38. As shown in Fig. 3a, splenocytes isolated from mice treated with Eph-NPs or Eph + CFA displayed stronger cytolytic activity against MC38 cells when compared with those immunized with EphA2-derived peptide alone, NP alone or PBS. Furthermore, splenocytes harvested from mice treated with Eph-NPs displayed a degree of anti-MC38 cytolytic activity equivalent to those immunized with Eph + CFA. On the other hand, the cytolytic activity was not observed against EphA2-negative BL6 cells in all treatment groups. We next examined whether lymphocytes isolated from the liver 1 day after tumor inoculation displayed cytolytic activity against a NK-sensitive cell, YAC-1 in vitro.

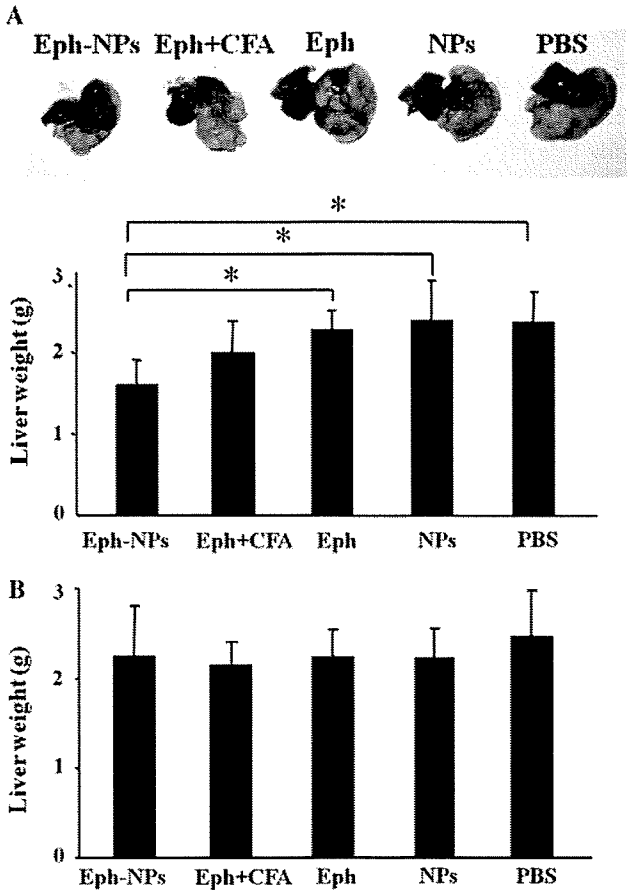

Fig. 2 Anti-tumor effects of immunization with Eph-NPs against liver tumor. C57BL/6 mice were immunized on day −7 and 0 with Eph-NPs, Eph + CFA, EphA2-derived peptide only (*Eph*), NPs only (*NPs*) or PBS. On day 0, 1×10^6 MC38 cells (**a**) or 1×10^6 BL6 cells (**b**) were injected intrahepatically. Fourteen days after immunization, mice were killed and liver weight was examined (**a** *upper panel*). Representative liver macroscopic view of each treatment group (**a** lower panel, **b**). Comparison of liver weight of each group. $*P < 0.05$. $N = 8$/group. Each data point represents the mean liver weight ± SD

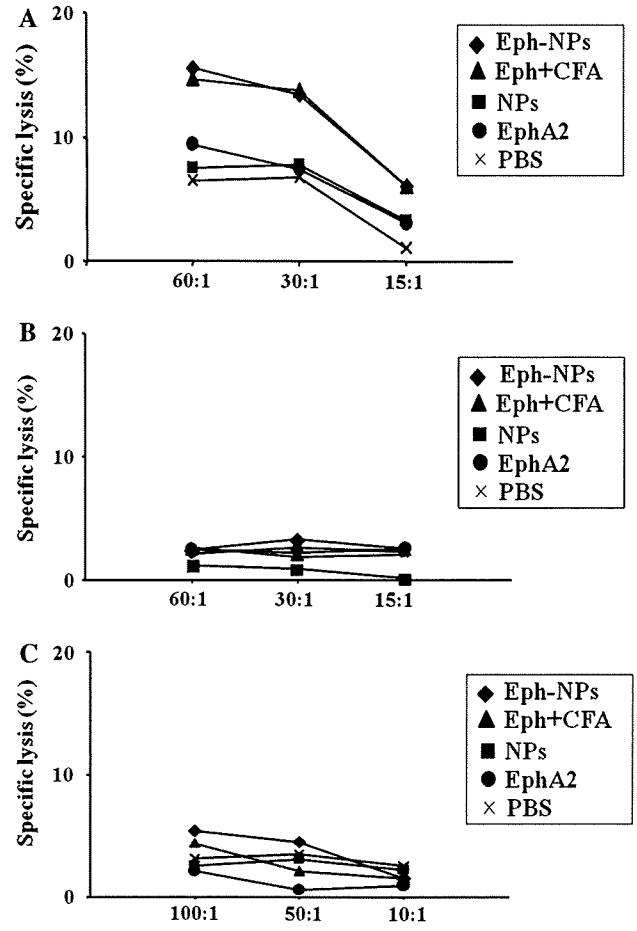

Fig. 3 Eph-NPs vaccines generated tumor-specific CTLs. Splenocytes were harvested from MC38 tumor-bearing mice 14 days after final treatment with Eph-NPs, Eph + CFA, NPs, Eph or PBS. Splenocytes were stimulated in vitro with MMC-treated MC38 cells for 5 days. The cytolytic activity of spleen cells was evaluated using 4-h ^{51}Cr release assays against MC38 (**a**) or irrelevant BL6 (**b**) tumor target cells at the indicated E:T ratios. **c** Liver lymphocytes were harvested 1 day after immunization into MC38-bearing mice. Liver lymphocytes were subjected to 4-h ^{51}Cr release assays against the NK-sensitive cells, YAC-1 as target cells at the indicated E:T ratios. Similar results were obtained in three independent experiments

No cytolytic activity was observed against a YAC-1 target cell in any of the control/treatment protocols (Fig. 3c). These results suggest that immunization using Eph-NPs or Eph + CFA effectively generated MC38-specific CTLs in vivo, which played essential roles in the liver tumor rejection.

Depletion of CD8+ T cells impairs the anti-tumor effects of immunization with Eph-NPs

To prove whether the therapeutic benefit associated with Eph-NPs vaccine in the MC38 liver tumor was dependent on CD4+, CD8+ T cells or NK cells, we performed selective cell subset depletion studies and C57BL/6 mice were immunized intraperioneally with Eph-NPs or PBS twice a week. On day 0, at the time of the second injection with these vaccines, mice were lightly anesthetized by isoflurane and 1×10^6 MC38 cells (EphA2-positive) were injected under the capsule of the left medial liver lobe as above. Mice were killed 14 days after tumor inoculation and the liver weight was measured. The anti-tumor efficacy of Eph-NPs immunization tended to be reduced in CD8+ T cell-depleted mice, while the liver weights of CD4+ T cell or NK cell-depleted mice were similar to those of non-depleted mice if the animals received Eph-NPs vaccines (Fig. 4). These results suggest that CD8+ T cells, but not CD4+ T cells or NK cells, tended to be required for optimal anti-tumor effects associated with Eph-NPs vaccines against liver tumor.

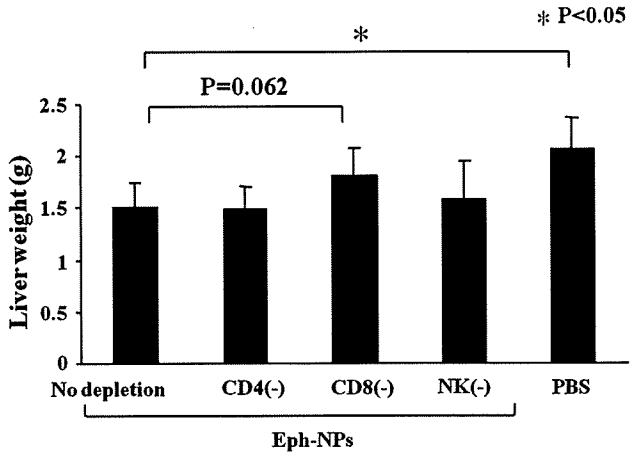

Fig. 4 Eph-NPs immunization tended to require CD8+ T cells, but not CD4+ T cells and NK cells in preventing liver tumor. Ab-mediated in vivo depletion of CD4+, CD8+ T cells, NK cells were performed (as described in "Materials and methods"), with the depleted mice then receiving Eph-NPs intraperitoneally (on day −7, 0) and 1×10^6 MC38 cells intrahepatically (day 0). Mice were killed 14 days after tumor inoculation and the liver weight was measured. $*P < 0.05$. $N = 8$/group. Each data point represents the mean liver weight ± SD

Safety of Eph-NPs versus Eph + CFA

To evaluate the safety of Eph-NPs vaccine, the serum ALT, TBil, Alb and Crnn were examined for mice immunized with Eph-NPs, Eph + CFA, Eph, NPs or PBS as above. Immunization with Eph + CFA induced liver damage as evidenced by elevated serum ALT levels compared with those for mice treated with PBS. In contrast, other treatments did not lead to liver damage. There was no toxic effect on TBil, Alb and Crnn in all treatment groups (Fig. 5). Immunization with CFA induced granulomatous peritonitis in all of the mice, but immunization with the other regimens did not. These results demonstrated that the Eph + CFA vaccine is toxic to hepatocytes but the Eph-NPs vaccine does not harm the liver or kidney.

Discussion

We created new biodegradable γ-PGA-Phe NPs for use as a new adjuvant [16]. Uto et al. [22] reported that γ-PGA-Phe NPs could activate DCs in vivo and cellular immunity

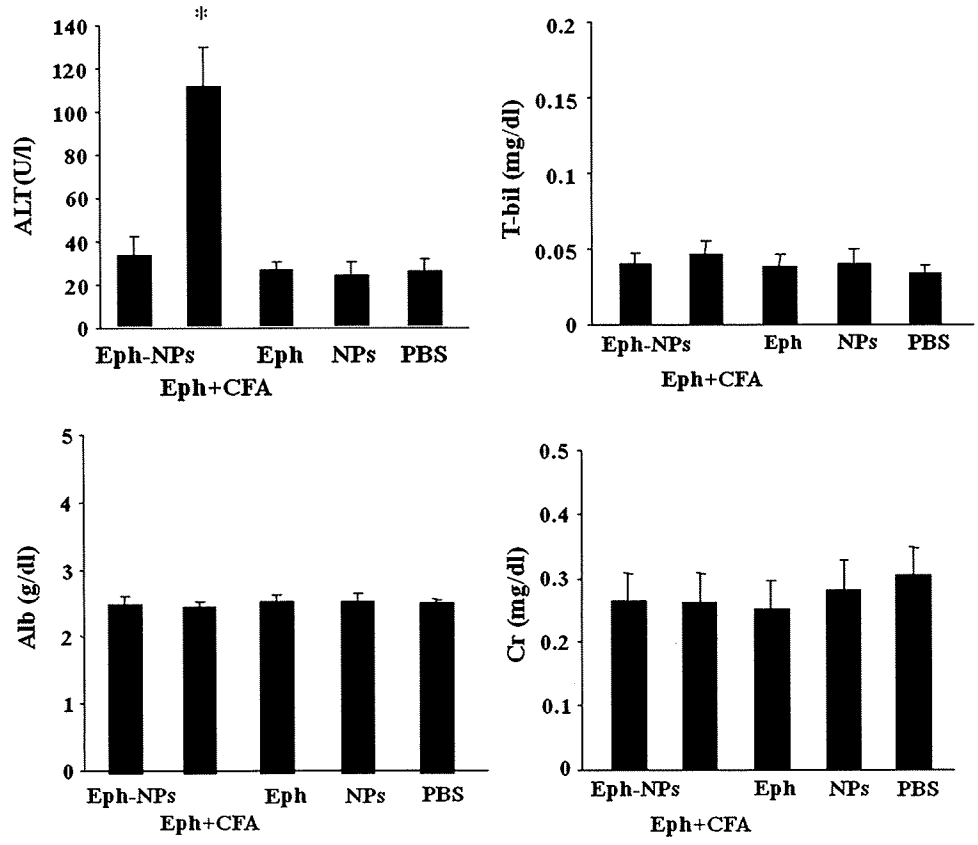

Fig. 5 Safety of Eph-NPs vaccine. Blood samples were obtained 7 days after final immunization of Eph-NPs, Eph + CFA, NPs, Eph or PBS. Levels of serum ALT, TBil, Alb or Crnn were examined. $N = 5$/group. $*P < 0.05$ versus PBS group

against tumor cells expressing artificial antigen OVA. All previous reports using γ-PGA-Phe NPs as a vaccine adjuvant were evaluated with OVA artificial antigen models [22, 29–31]. Dhodapkar et al. [32] reported that the immunogenicity of peptides derived from self-melanoma antigens were very weak compared with viral protein-derived peptides. Although many TAA-derived peptides may be applicable to clinical use as peptide-based vaccines, most TAAs are self-antigens and not or weakly immunogenic, which is inferior to elicit enough anti-tumor immunity. Thus, the anti-tumor effect of γ-PGA-Phe NPs vaccines should be reevaluated by using self-TAA-derived peptides. In this study, we used EphA2-derived peptide [25] as a self-TAA. EphA2 is of particular interest due to evidence suggesting its involvement in carcinogenesis. EphA2 is a 130 kDa protein normally localized to sites of cell-to-cell contact, where it plays a role in contact growth inhibition [33]. However, cellular overexpression of EphA2, either as a result of its constitutive dysregulation or ectopic gene insertion, results in the disruption of cell-to-cell contacts, and enhancement of cell-to-extracellular matrix attachments [33]. As a result, tumor cells that overexpress EphA2 exhibit increased motility and invasive properties, consistent with a pro-metastatic phenotype [33]. Overexpression of EphA2 has been observed in numerous cancer types [34], including melanoma [35] and carcinomas of the breast [36, 37], lung [38], pancreas [39] and prostate [40]. We demonstrated the usefulness of Eph-NPs vaccine therapy, which revealed the future potential of clinical applications of this treatment in various cancers.

Complete Freund's adjuvant is an emulsion of water and mineral containing killed mycobacteria and has highly potent activity as an adjuvant. However, CFA administration induces adverse effects such as weight loss, neutrophilia and granulomatous peritonitis [41–43]. Consistent with earlier observations, immunization with Eph + CFA induced liver hepatocyte damage evidenced by elevation of ALT levels and granulomatous peritonitis in all of the mice. We demonstrated that immunization with Eph-NPs revealed anti-tumor effects against liver tumor via the generation of acquired immunity equal to the strongest but very toxic adjuvant, CFA, suggesting that our biodegradable γ-PGA-Phe NPs could be a promising candidate for a vaccine adjuvant against liver cancer.

IFN-γ ELISPOT assays revealed that immunization with Eph-NPs into normal mice resulted in induction of EphA2-derived peptide-specific CD8+ T cells at a level equivalent to Eph + CFA vaccine. Based on these results, we examined the anti-tumor effect of Eph-NPs vaccines in the EphA2-positive MC38 liver tumor model. The Eph-NPs vaccines resulted in eliciting anti-tumor effects against EphA2-positive MC38 liver tumor, but not against EphA2-negative BL6 melanoma, suggesting that EphA2-specific anti-tumor immunity was generated by Eph-NPs vaccines, which is consistent with our IFN-γ ELISPOT assay data. These results suggested that the anti-tumor potential of γ-PGA-Phe NPs vaccine is similar to that of CFA as an adjuvant in peptide-based vaccine. Importantly, Eph-NPs vaccine showed no toxic side effect on liver and kidney function. In contrast, CFA + Eph vaccine caused liver damage. γ-PGA-Phe NPs vaccine is safe and should be clinically applicable. This supports the clinical potential of γ-PGA-Phe NPs vaccine in cancer treatment.

In vitro cytotoxicity assays revealed that the anti-tumor effector cells for killing MC38 cells were CD8+ T cells, and possibly CTLs. This cytolytic activity was specific for MC38 cells because splenocytes did not kill BL6 cells. These results suggested that Eph-NPs vaccines could efficiently generate specific CTLs that recognize and kill relevant EphA2-positive, but not irrelevant EphA2-negative tumor targets. The liver uniquely contains an abundance of not only T cells, but also NK cells and NKT cells when compared with other organs [44, 45]. We have previously reported that not only CD8+ T cells, but also NK cells are required for optimal anti-tumor effects associated with EphA2-derived peptide pulsed DCs vaccines in liver tumors [26]. In this study, liver NK cells were not activated by Eph-NPs vaccination. Spleen NK cells were also not activated by Eph-NPs vaccine, and naïve spleen cells co-cultured with γ-PGA-Phe NPs or Eph-NPs could not display cytolytic activity against YAC-1 targets (S. Yamaguchi et al., unpublished data). These results suggested that the Eph-NPs vaccine could activate acquired immunity specifically. Our in vivo lymphocyte depletion studies demonstrated that CD8+ T cells, not CD4+ T cells and NK cells, tended to contribute to the inhibition of liver tumor growth in Eph-NPs vaccine, although we could not deny the possibility that humoral immune responses against EphA2 may also be generated by Eph-NPs vaccine. Previous reports demonstrated that biodegradable NPs were taken up by dedicated professional antigen-presenting cells, such as DCs, which resulted in their subsequent migration to lymph nodes, increased production of cytokines, and enhanced expression of costimulatory molecules followed by antigen-presentation to T cells [22, 29, 30]. Eph-NPs taken by DCs were directly presented to T cells and the generated Eph-specific CD8+ CTL could serve as effector cells against EphA2 expressing MC38 tumor.

In spite of recent progress and early success reported for adjuvant peptide vaccine trials in the prevention of liver cancer, there remains a great need to develop novel and effective treatment modalities. In this study, we demonstrated that immunization with Eph-NPs vaccines revealed anti-tumor effects against liver cancers via acquired immunity equivalent to the strongest CFA and that Eph-NPs vaccines did not lead liver or kidney damage. These results

suggest that γ-PGA-Phe NPs could be a promising candidate for a vaccine adjuvant against liver cancer. We are now preparing for the clinical application of γ-PGA-Phe NPs-peptide vaccine against liver cancer.

Acknowledgments This work was supported by a Grant-in-Aid from Core Research for Evolutional Science and Technology (CREST) from Japan Science and Technology Agency (JST).

References

1. Berzofsky JA, Ahlers JD, Belyakov IM (2001) Strategies for designing and optimizing new generation vaccines. Nat Rev Immunol 1:209–219
2. Schijns VE (2000) Immunological concepts of vaccine adjuvant activity. Curr Opin Immunol 12:456–463
3. Valmori D, Souleimanian NE, Tosello V et al (2007) Vaccination with NY-ESO-1 protein and CPG in Montanide induces integrated antibody/Th1 responses and CD8 T cells through cross-priming. Proc Natl Acad Sci USA 104:8947–8952
4. Wang F, Bade E, Kuniyoshi C et al (1999) Phase 1 trial of a MART-1 peptide vaccine with incomplete Freund's adjuvants for resected high-risk melanoma. Clin Cancer Res 5:2756–2765
5. Gilewski TA, Ragupathi G, Dickler M et al (2007) Immunization of high-risk breast cancer patients with clustered sTn-KLH conjugate plus the immunologic adjuvant QS-21. Clin Cancer Res 13:2977–2985
6. Bottomley A, Debruyne C, Ferip E et al (2008) Symptom and quality of life results of an international randomized phase 3 study of adjuvant vaccination with Bec2/BCG in responding patients with limited disease small-cell lung cancer. Eur J Cancer 44:2178–2184
7. Perales MA, Yuan J, Powel S et al (2008) Phase 1/2 study of GM-CSF DNA as an adjuvant for a multipeptide cancer vaccine in patients with advanced melanoma. Mol Ther 16:2022–2029
8. Mocellin S, Riccardo-Rossi C, Lise M et al (2004) Colorectal cancer vaccines: principles, results, and perspectives. Gastroenterology 27:1821–1837
9. Dinauer N, Balthasar S, Weber C et al (2005) Selective targeting of antibody-conjugated nanoparticles to leukemic cells and primary T-lymphocytes. Biomaterials 26:5898–5906
10. Khatri K, Goyal AK, Gupta N et al (2008) Plasmid DNA loaded chitosan nanoparticles for nasal mucosal immunization against hepatitis B. Int J Pharm 354:235–241
11. Almeida AJ, Souto E (2007) Solid lipid nanoparticles as a drug delivery system for peptides and proteins. Adv Drug Deliv Rev 59:478–490
12. Hayakawa T, Kawamura M, Okamoto M et al (1998) Concanavalin A-immobilized polystyrene nanospheres capture HIV-1 and gp120: potential approach towards prevention of viral transmission. J Med Virol 56:327–331
13. Kawamura M, Naito T, Ueno M et al (2002) Induction of mucosal IgA following intravaginal administration of inactivated HIV-1-capturing nanospheres in mice. J Med Virol 66:291–298
14. Akagi T, Kawamura M, Ueno M et al (2003) Mucosal immunization with inactivated HIV-1-capturing nanospheres induces a significant HIV-1-specific vaginal antibody response in mice. J Med Virol 69:163–172
15. Miyake A, Akagi T, Enose Y et al (2004) Induction of HIV-specific antibody response and protection against vaginal SHIV transmission by intranasal immunization with inactivated SHIV-capturing nanospheres in macaques. J Med Virol 73:368–377
16. Akagi T, Wang X, Uto T, Baba M, Akashi M (2007) Protein direct delivery to dendritic cells using nanoparticles based on amphiphilic poly(amino acid) derivatives. Biomaterials 28:3427–3436
17. Shih IL, Van YT (2001) The production of poly-(γ-glutamic acid) from microorganisms and its various applications. Bioresour Technol 79:207–225
18. Obst M, Steinbüchel A (2004) Microbial degradation of poly(amino acid)s. Biomacromolecules 5:1166–1176
19. Sung MH, Park C, Kim CJ, Poo H, Soda K, Ashiuchi M (2005) Natural and edible biopolymer poly-γ-glutamic acid: synthesis, production, and applications. Chem Rec 5:352–366
20. Akagi T, Higashi M, Kaneko T et al (2005) In vitro enzymatic degradation of nanoparticles prepared from hydrophobically-modified poly(γ-glutamic acid). Macromol Biosci 14:598–602
21. Akagi T, Kaneko T, Kida T, Akashi M (2006) Multifunctional conjugation of proteins on/into bio-nanoparticles prepared by amphiphilic poly(γ-glutamic acid). J Biomater Sci Polym Ed 17:875–892
22. Uto T, Wang X, Sato K et al (2007) Targeting of antigen to dendritic cells with poly(gamma-glutamic acid) nanoparticles induces antigen-specific humoral and cellular immunity. J Immunol 178:2979–2986
23. Olson RM, Perencevich NP, Malcolm AW et al (1980) Patterns of recurrence following curative resection of adenocarcinoma of the colon and rectum. Cancer 45:2969–2974
24. Malcolm AW, Perencevich NP, Olson RM et al (1981) Analysis of recurrence patterns following curative resection for carcinoma of the colon and rectum. Surg Gynecol Obstet 152:131–136
25. Yamaguchi S, Tatsumi T, Takehara T et al (2007) Immunotherapy of murine colon cancer using receptor tyrosine kinase EphA2-derived peptide-pulsed dendritic cell vaccines. Cancer 110:1469–1477
26. Yamaguchi S, Tatsumi T, Takehara T et al (2008) Dendritic cell-based vaccines suppress metastatic liver tumor via activation of local innate and acquired immunity. Cancer Immunol Immunother 57:1861–1869
27. Akagi T, Kaneko T, Kida T et al (2005) Preparation and characterization of biodegradable nanoparticles based on poly(γ-glutamic acid) with L-phenylalanine as a protein carrier. J Control Release 108:226–236
28. Tatsumi T, Gambotto A, Robbins PD et al (2002) Interleukin 18-gene transfer expands the repertoire of anti-tumor Th1-type immunity elicited by dendritic cell- based vaccines in association with enhanced therapeutic efficacy. Cancer Res 62:5853–5858
29. Yoshikawa T, Okada N, Oda A et al (2008) Development of amphiphilic γ-PGA-nanoparticle based tumor vaccine: potential of the nanoparticle cytosolic protein delivery carrier. Biochem Biophys Res Commun 366:408–413
30. Yoshikawa T, Okada N, Oda A et al (2008) Nanoparticles built by self-assembly of amphiphilic γ-PGA can deliver antigens to antigen-presenting cells with high efficiency: a new tumor-vaccine carrier for eliciting effector T cells. Vaccine 26:1303–1313
31. Uto T, Wang X, Akagi T et al (2009) Improvement of adaptive immunity by antigen-carrying biodegradable nanoparticles. Biochem Biophys Res Commun 379:600–604413
32. Dhodapkar MV, Young JW, Chapman PB et al (2006) Paucity of functional T-cell memory to melanoma antigens in healthy donors and melanoma patients. Clin Cancer Res 6:4831–4838
33. Zantek ND, Azimi M, Fedor-Chaiken M, Wang B, Brackenbury R, Kinch MS (1999) E-cadherin regulates the function of the EphA2 receptor tyrosine kinase. Cell Growth Differ 10:629–638
34. DeRisi J, Penland L, Brown PO et al (1996) Use of a cDNA microarray to analyse gene expression patterns in human cancer. Nat Genet 14:457–460

35. Easty DJ, Hill SP, Hsu MY et al (1999) Up-regulation of ephrin-A1 during melanoma progression. Int J Cancer 84:494–501
36. Lu M, Miller KD, Gokmen-Polar Y, Jeng MH, Kinch MS (2003) EphA2 overexpression decreases estrogen dependence and tamoxifen sensitivity. Cancer Res 63:3425–3429
37. Zelinski DP, Zantek ND, Stewart JC, Irizarry AR, Kinch MS (2001) EphA2 overexpression causes tumorigenesis of mammary epithelial cells. Cancer Res 61:2301–2306
38. Branan JM, Dong W, Prudkin L et al (2009) Expression of the receptor tyrosine kinase EphA2 is increased in smokers and predicts poor survival in non-small cell lung cancer. Clin Cancer Res 15:4423–4430
39. Duxbury MS, Ito H, Zinner MJ, Ashley SW, Whang EE (2004) EphA2: a determinant of malignant cellular behavior and a potential therapeutic target in pancreatic adenocarcinoma. Oncogene 23:1448–1456
40. D'Amico TA, Aloia TA, Moore MB et al (2001) Predicting the sites of metastases from lung cancer using molecular biologic markers. Ann Thorac Surg 72:1144–1148
41. Broderson JR (1989) A retrospective review of lesions associated with the use of Freund's adjuvant. Lab Anim Sci 39:400–405
42. Amyx HL (1987) Control of animal pain and distress in antibody production and infectious disease studies. J Am Vet Med Assoc 191:1287–1289
43. Toth LA, Dunlap AW, Olson GA et al (1989) An evaluation of distress following intraperitoneal immunization with Freund' adjuvant in mice. Lab Anim Sci 39:122–126
44. George AP, Catherine AP (2005) Liver immunobiology. Toxicol Pathol 33:52–62
45. Doherty DG, O'Farrelly C (2000) Innate and adaptive lymphoid cells in human liver. Immunol Rev 174:5–20

Cancer Immunol Immunother (2010) 59:453–463
DOI 10.1007/s00262-009-0764-x

ORIGINAL ARTICLE

Natural killer cell is a major producer of interferon γ that is critical for the IL-12-induced anti-tumor effect in mice

Akio Uemura · Tetsuo Takehara · Takuya Miyagi · Takahiro Suzuki · Tomohide Tatsumi · Kazuyoshi Ohkawa · Tatsuya Kanto · Naoki Hiramatsu · Norio Hayashi

Received: 12 February 2009 / Accepted: 24 August 2009 / Published online: 16 September 2009

Abstract Although the anti-tumor effect of IL-12 is mediated mostly by IFNγ, which cell types most efficiently produce IFNγ and therefore initiate or promote the anti-tumor effect of IL-12 has not been clearly determined. In the present study, we demonstrated hydrodynamic injection of the IL-12 gene led to prolonged IFNγ production, NK-cell activation and complete inhibition of liver metastasis of CT-26 colon cancer cells in wild-type mice, but not in IFNγ knockout mice. NK cells expressed higher levels of STAT4 and upon IL-12 administration displayed stronger STAT4 phosphorylation and IFNγ production than non-NK cells. Adoptive transfer of wild-type NK cells into IFNγ knockout mice restored IL-12-induced IFNγ production, NK-cell activation and anti-tumor effect, whereas transfer of the same number of wild-type non-NK cells did not. In conclusion, NK cells are predominant producers of IFNγ that is critical for IL-12 anti-tumor therapy.

Keywords IFNγ · Innate immunity · Liver tumor · IL-12 · NK

A. Uemura and T. Takehara contributed equally to this work.

Electronic supplementary material The online version of this article (doi:10.1007/s00262-009-0764-x) contains supplementary material, which is available to authorized users.

A. Uemura · T. Takehara · T. Miyagi · T. Suzuki · T. Tatsumi · K. Ohkawa · T. Kanto · N. Hiramatsu · N. Hayashi (✉)
Department of Gastroenterology and Hepatology,
Osaka University Graduate School of Medicine,
2-2 Yamada-oka, Suita, Osaka 565-0871, Japan
e-mail: hayashin@gh.med.osaka-u.ac.jp

A. Uemura
e-mail: akioue@gh.med.osaka-u.ac.jp

Introduction

IL-12 is a 70-kDa heterodimer protein, composed of p35 and p40 subunits, mainly produced by antigen-presenting cells. IL-12 was originally found as a "natural killer-stimulating factor" and a "cytotoxic lymphocyte maturation factor" [1, 2]. IL-12 has multi-potent effects, inducing a Th1 response, enhancing the CD8 T-cell response, activating natural killer cells and inducing production of IFNγ [3, 4]. Therapeutic use of IL-12, either using its recombinant protein or gene, can induce an efficient anti-tumor effect on primary or metastatic tumors in various murine models and humans [5, 6].

Research has shown that IL-12 mediates anti-tumor effects in a variety of ways. They include anti-proliferative effects, anti-angiogenic effects [7, 8] and cytotoxic effects of effector lymphocytes. A variety of effector cells has been reported to be required for IL-12-mediated anti-tumor effects: they include CD8 T cells [9], NKT cells [10], CD4 T cells [11] and NK cells [12]. The relative contribution of these cells may differ among IL-12 doses and types of tumor models [13]. Endogenous IFNγ production is required for most, if not all, of the anti-tumor effects of IL-12 administration [14, 15]. IL-12 stimulates a variety of immune cells, such as T cells [16], B cells [17] and NK cells [18], to produce IFNγ. However, which cell types are most critical for producing IFNγ during IL-12 therapy is not clearly known.

In the present study, we used a murine model of liver metastasis of CT-26 colon cancer cells and found that NK cells highly expressed the IL-12 signaling molecule STAT4 and most efficiently produced IFNγ. IFNγ was essential for the anti-tumor effect of IL-12, and NK-cell production of IFNγ sufficed to produce the full-blown anti-tumor effects. These results demonstrated that NK cells

serve not only as an effector but also as an important mediator producing IFNγ that is critical for the anti-tumor effects of IL-12.

Materials and methods

Mice

Specific pathogen-free female Balb/c mice were purchased from Clea Japan, Inc (Tokyo, Japan). Rag2 knockout (Rag2 KO) mice with a Balb/c background were purchased from Taconic (Germantown, NY). IFNγ knockout (GKO) mice with a Balb/c background were kindly provided by Dr. Yoichiro Iwakura (Institute of Medical Science, University of Tokyo). All mice used were at the age of 6 to 10 weeks. They were housed under conditions of controlled temperature and light with free access to food and water at the Institute of Experimental Animal Science, Osaka University Graduate School of Medicine. All animals received humane care, and the study protocol complied with the institution's guidelines.

Tumor models

Intra-splenic injection of tumor cells was used to establish micro-disseminated liver tumors in mice [19]. CT-26 colon cancer cells originating from Balb/c mice were maintained in RPMI1620 supplemented with 10% FCS. Syngeneic mice were anesthetized with pentobarbital and given a cut on the left side flank. CT-26 cells (1×10^5) were suspended in 200 μl of PBS and injected into the spleen.

Injection of naked plasmid DNA

A plasmid coding the murine IL-12 gene, pCMV-IL-12, was generously provided by Dr. M Watanabe (Laboratory of Experimental Immunology, Division of Basic Sciences, National Cancer Institute-Frederick Cancer Research and Development Center) [20]. Plasmid DNA was prepared using an EndoFree plasmid system (Qiagen, Hilden, Germany,) according to the manufacturer's instructions. Hydrodynamic injection of plasmid DNA was performed as previously described [21]. In brief, 25 μg of plasmid DNA was diluted with 2.0 ml of lactated Ringer's solution and injected into the tail vein, using a syringe with a 26-gauge needle. DNA injection was completed within 5 to 8 s.

ELISA

Blood samples were serially obtained from the venous plexus in the retro-orbita under light anesthesia. The levels of serum IL-12 p70, IFNγ (BD Biosciences-Pharmingen, San Diego, CA), IFNγ-inducible protein 10 (IP-10) and monokine induced by IFNγ (MIG) (R&D Systems, Inc, Minneapolis, MN) were measured using commercially available ELISA kits in accordance with the manufacturer's instructions.

Mononuclear cells

Mononuclear cells were isolated from the liver or spleen as previously described. The NK activity of mononuclear cells was assessed by a standard 4-h ^{51}Cr-releasing assay using Yac1 cells as targets. In some experiments, mononuclear cells were separated into $DX5^+$ cells (NK cells) and $DX5^-$ cells (non-NK cells) using the MACS system (Miltenyi Biotec GmbH, Bergisch Gladbach, Germany). The purity of the isolated NK-cell population was found to be greater than 90% by FACS analysis.

Flow cytometric analysis

Liver mononuclear cells were isolated 2 days after pCMV-IL-12 injection. Cytokine secretion was then blocked by the addition of brefeldin A for 4 h. Next, liver mononuclear cells were stained with FITC-conjugated anti-TCRβ antibody and biotin-conjugated anti-CD49b antibody (DX5), fixed and permeabilized with Cytofix/Cytoperm (BD Biosciences), and stained with PE-conjugated anti-INFγ antibody or corresponding isotype controls. Analysis was performed using a FACSCalibur (Becton Dickinson), with the resulting data analyzed using the CELLQuest program (Becton Dickinson). NK cells were identified as $DX5^+/TCR\beta^-$ lymphocytes, NKT cells as $DX5^+/TCR\beta^+$ lymphocytes and T cells as $DX5^-/TCR\beta^+$ lymphocytes.

Adoptive transfer

For adoptive transfer experiments, GKO mice were injected intravenously 1 day before plasmid DNA injection with 2.0×10^8 whole mononuclear cells or 4.0×10^6 NK cells, or non-NK cells or whole mononuclear cells, all of which had been harvested from wild-type mice that can produce IFNγ.

Western blotting

Mouse recombinant IL-12 was purchased from R&D Systems, Inc (Minneapolis, MN). Mononuclear cells were treated with or without IL-12. Whole cell lysate was prepared from mononuclear cells from mice, and 20 μg of protein was separated by SDS-PAGE and transferred to the PVDF membrane. The membrane was stained with anti-STAT4 antibody (BD biosciences),

anti-phospho-specific STAT4 (pY693) antibody (BD biosciences), anti-STAT1 antibody (Cell Signaling), anti-phospho-specific STAT1 antibody (Cell Signaling) and visualized by chemiluminescence.

NK-cell depletion

For depletion of NK cells in vivo, anti-asialoGM1 antibody (WAKO, Osaka, Japan) was intraperitoneally administered. We determined the appropriate dosing to be 500 μg/mouse (50 μl when dissolved according to the manufacturer's instructions) based on FACS analysis of hepatic mononuclear cells. The percentage of $DX5^+/TCR\beta^-$ cells (NK cells) is 12.6 ± 2.4% in IgG-injected liver, whereas it decreased to 0.76 ± 0.04% one day after anti-asialo GM1 antibody injection ($N = 3$/group). This effect remained at least 3 days after anti-asialo GM1 antibody injection. NKT cells were less affected than NK cells, because 90% of $DX5^+/TCR\beta^+$ cells (NKT cells) still remained in the liver after the treatment. Anti-asialoGM1 antibody was injected 1 day after tumor inoculation and then every 5 days. For the control, the same amount of normal rabbit immunoglobulin (DAKO, Copenhagen, Denmark) was intraperitoneally administered.

Histology

The formalin-fixed livers were paraffin-embedded, and liver sections were analyzed by hematoxylin-eosin staining. Acetone-fixed fresh frozen liver sections were immunostained with anti-mouse CD4 (H123.19), anti-mouse CD8α (53-6.7) or anti-CD31 (390) monoclonal antibody (all from BD Biosciences), using a VECSTAIN ABC kit (Vector Laboratories, Burlingame, California, USA).

Statistics

Data are represented as mean ± SD. Comparisons between groups were analyzed by unpaired t-test with Welch's correction. $p < 0.05$ was considered statistically significant.

Results

Hydrodynamic injection of IL-12-expressing plasmid led to prolonged production of IFNγ

Hydrodynamics-based gene delivery into mice establishes efficient foreign gene expression predominantly in the liver, especially in hepatocytes. Serial measurement of serum IL-12 demonstrated that pCMV-IL-12 injection led to substantial IL-12 production on day 1. The levels of serum IL-12 then rapidly declined (Fig. 1a). We also measured IFNγ production in serum, since IL-12 is known to activate IFNγ production. pCMV-IL-12 and, to a lesser extent, pCMV injection increased serum IFNγ on day 1. In contrast to the pCMV injection group, high levels of serum IFNγ were maintained at later time points in the pCMV-IL-12 injection group (Fig. 1a). Thus, hydrodynamic injection of pCMV-IL-12 led to prolonged production of IFNγ. Transient IFNγ production followed by control plasmid may be an indirect effect of liver injury caused by bolus injection of saline or DNA injection.

IL-12 therapy induced NK activation and anti-metastatic effects, both of which are critically dependent on IFNγ

To examine the biological effects of the produced IL-12, we evaluated the NK activity of mononuclear cells from the liver. pCMV-IL-12 injection, but not control pCMV injection, increased Yac1 lytic activity of hepatic mononuclear cells (Fig. 1b). When GKO mice were injected with pCMV-IL-12 or pCMV, the hepatic mononuclear cells did not display any lytic ability to Yac1 cells, suggesting that IL-12-mediated NK-cell activation required IFNγ.

To examine the anti-metastatic effect of IL-12, pCMV-IL-12 or pCMV was injected into wild-type mice 2 days after intrasplenic injection of CT-26 cells. At 14 days after tumor injection, the mice were killed for evaluation of liver tumor (Fig. 1c). While pCMV-injected mice displayed huge liver tumors, pCMV-IL-12-injected mice did not show any macroscopic or microscopic tumor (Fig. 1d). Liver weight was significantly higher in pCMV-injected mice than pCMV-IL-12-injected mice, reflecting liver tumor formation. To examine the involvement of IFNγ in the IL-12-induced anti-tumor effect, we injected pCMV or pCMV-IL-12 into GKO mice 2 days after CT-26 injection. At 14 days after CT-26 injection, both groups showed similar degrees of tumor formation and there was no significant difference in liver weight between the two. This indicated that IL-12-induced anti-metastatic effect was strictly dependent on IFNγ.

NK cells were the most potent producer of IFNγ during IL-12 therapy

To evaluate which cell types most efficiently produced IFNγ, we isolated hepatic mononuclear cells from mice 2 days after plasmid injection and then stained cell surface TCRβ and DX5 as well as intracellular IFNγ (Fig. 2). $TCR\beta^-/DX5^+$ NK cells, $TCR\beta^+/DX5^+$ NKT cells and $TCR\beta^+/DX5^-$ T cells from pCMV-IL-12-injected mice showed significant levels of IFNγ production compared

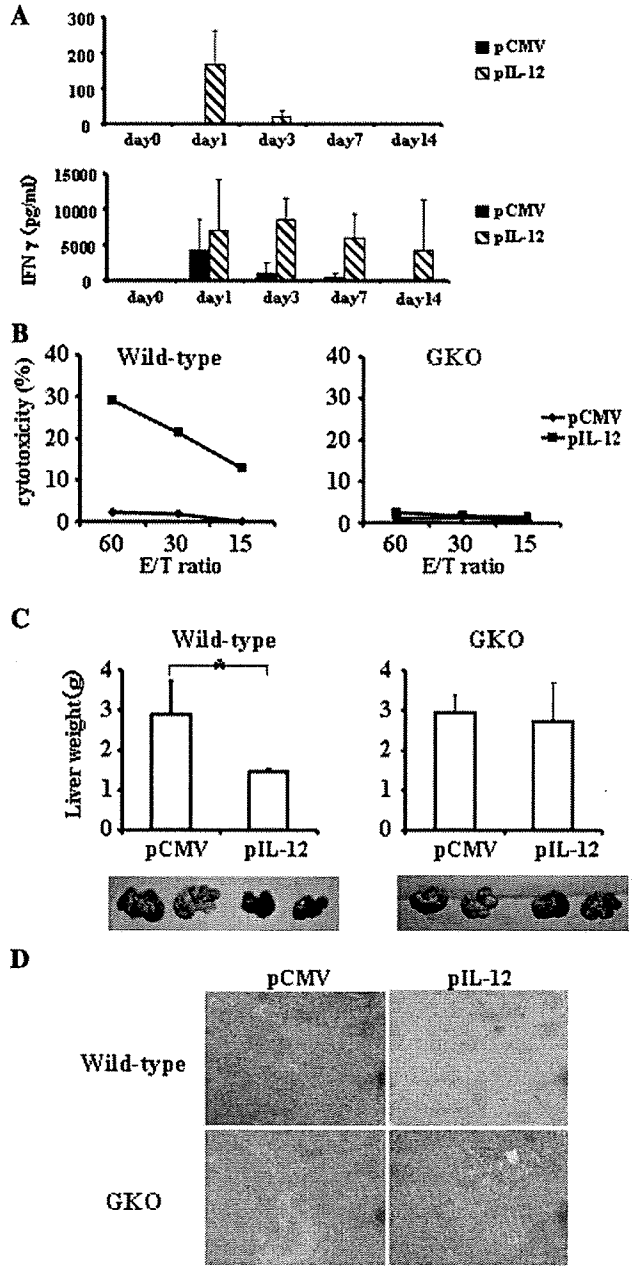

Fig. 1 Effects of hydrodynamic injection of IL-12-encoding plasmid. **a** Wild-type mice were hydrodynamically injected with either pCMV-IL-12 (*hatched bars*) or pCMV (*closed bars*) and bled at the indicated time points to measure the levels of serum IL-12 and IFNγ. Results are indicated as mean and SD ($n = 6$/group). **b** NK-cell activation after IL-12 administration. Hepatic mononuclear cells were isolated from wild-type mice (*left*) or GKO mice (*right*) which had been injected with pCMV-IL-12 (*closed squares*) or pCMV (*closed diamonds*) 4 days earlier. Yac1 lytic ability was measured by a standard ^{51}Cr-release assay at the indicated effector and target ratios (E/T ratio). All experiments were performed at least 3 times and representative data are shown. **c** and **d** Anti-metastatic effects of IL-12 therapy. Wild-type mice (*left*) or GKO mice (*right*) were intrasplenically injected with CT-26 cells and, 2 days later, hydrodynamically injected with either pCMV-IL-12 or pCMV. At 14 days after the plasmid injection, the mice were killed to examine liver tumor development. **c** Data are indicated as mean and SD of the liver weight at the top ($n = 6$/group) and a representative picture of the liver in each group is shown at the bottom. $^*p < 0.001$. **d** Representative histology of liver sections

with those from naive mice or pCMV-injected mice. The levels of IFNγ production were highest in NK cells among those cells. Even at a later time point, 7 days after plasmid injection, NK cells were found to produce the highest levels of IFNγ (data not shown).

IL-12-induced STAT4 signaling and IFNγ production increased in NK cells

IL-12 activates Janus kinases Tyk2 and Jak2, STAT4 as well as other STATs. To examine the activation of STAT1 and STAT4, we isolated splenocytes from wild-type mice and GKO mice and stimulated them with IL-12 and/or IFNγ in the presence or absence of anti-IFNγ Ab (Fig. 3a). IL-12 led to phosphorylation of both STAT1 and STAT4 in wild-type splenocytes. In contrast, the same treatment led to phosphorylation of STAT4, but not of STAT1, in GKO splenocytes. Addition of IFNγ restored STAT1 phosphorylation in GKO splenocytes. Furthermore, adding anti-IFNγ inhibited STAT1 phosphorylation in wild-type cells. These findings demonstrated that phosphorylation of STAT4 is a direct effect of IL-12 but phosphorylation of STAT1 is indirect, via an autocrine or paracrine IFNγ-dependent manner.

To examine STAT1 and STAT4 activation and IFNγ production in NK cells and non-NK cells, we prepared whole mononuclear cells as well as NK and non-NK populations from wild-type spleens and stimulated the cells with IL-12 (Fig. 3b). NK cells expressed higher levels of STAT4 than non-NK cells. Upon IL-12 treatment, STAT4 was rapidly phosphorylated in NK cells, but to a lesser extent in non-NK cells. In contrast, NK cells expressed lesser levels of STAT1 than non-NK cells. STAT1 was similarly phosphorylated in NK cells and non-NK cells upon IL-12 treatment. Both NK cells and non-NK cells produced significant levels of IFNγ, but the levels were much higher in NK cells than non-NK cells (Fig. 3c). These results indicated that compared with non-NK cells, NK cells possessed higher levels of STAT4, a direct signaling molecule of IL-12, and produced higher levels of IFNγ than non-NK cells.

NK cells were sufficient for IL-12-mediated anti-tumor effects

The above observation indicated that NK cells are a predominant producer of IFNγ, which was critical for the IL-12-induced anti-tumor effects. To examine whether NK

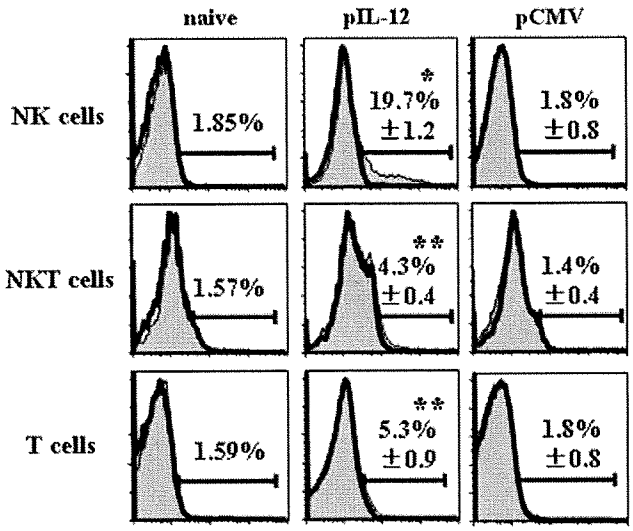

Fig. 2 IFNγ expression of mononuclear cells after IL-12 administration. Wild-type mice were injected with pCMV-IL-12 or pCMV, or were untreated (naive). Mononuclear cells were isolated from the liver 2 days after plasmid injection and stained with anti-TCRβ mAb, anti-DX5 mAb and anti-IFNγ mAb. *Closed histograms* show the IFNγ expression in the gated populations ($TCR\beta^-/DX5^+$ cells for NK cells, $TCR\beta^+/DX5^+$ cells for NKT cells and $TCR\beta^+/DX5^-$ cells for T cells). Isotype control stainings are shown by *open histograms*. Numbers in histograms represent averages ± SD of percentages of positive cells ($n = 3$ mice/group). $^*p < 0.0001$ vs. mock in NK populations. $^{**}p < 0.05$ vs. mock in each population

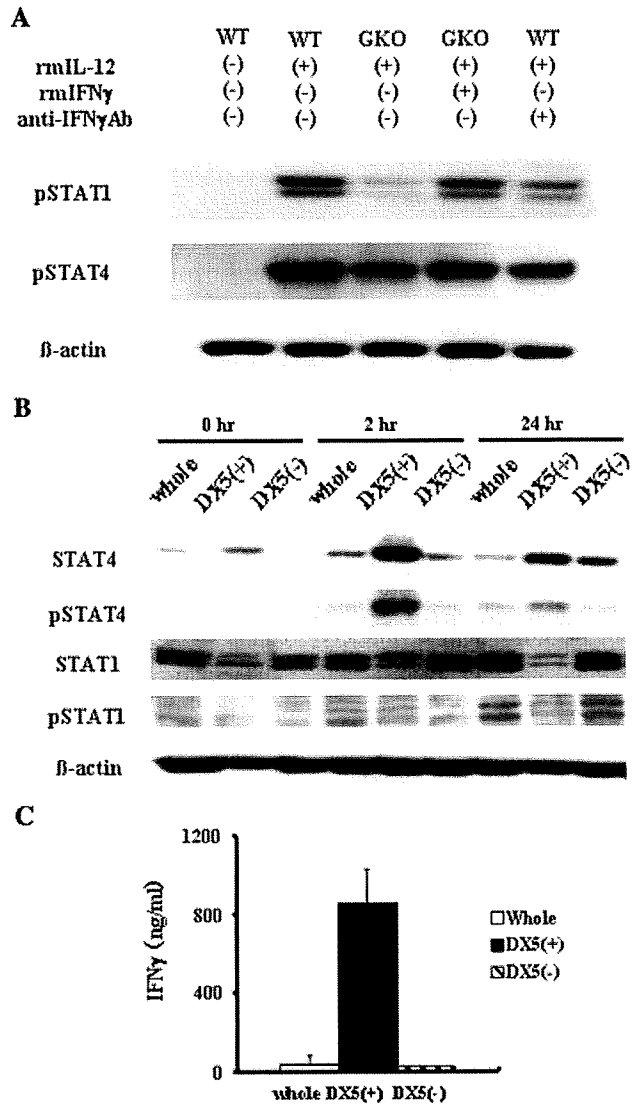

Fig. 3 STAT signaling and IFNγ production of mononuclear cells in vitro treated with IL-12. **a** STAT1 and STAT4 activation of splenocytes in vitro treated with IL-12. Splenocytes were isolated from wild-type mice or GKO mice and treated with or without recombinant IL-12 (20 ng/mL) in the presence or absence of recombinant IFNγ (500 ng/mL) or anti- IFNγ antibody (20 μg/mL) for 24 h. Cellular lysates were analyzed by Western blot for the expression of phospho-STAT1, phospho-STAT4 and β-actin. **b** and **c** STATs expression and signaling of NK cells and non-NK cells. Splenocytes were isolated from wild-type mice. Whole splenocytes were further purified into $DX5^+$ cells and $DX5^-$ cells. Each cell population was cultured with recombinant IL-12 (20 ng/mL) for the indicated times. **b** The cells were lysed to examine expression of whole STAT and phospho-STAT by Western blot. **c** The levels of IFNγ in the culture supernatant at 24 h were determined by ELISA. Data are expressed as mean and SD ($n = 3$)

cells are sufficient for the anti-metastatic effects of IL-12, we examined the anti-metastatic effect in Rag2 KO mice which lack T cells, B cells and NKT cells. pCMV-IL-12 injection enhanced the Yac1 lytic ability of hepatic mononuclear cells in Rag2 KO mice higher than in wild-type mice (Fig. 4a). To examine whether NK cells are sufficient for IL-12-mediated rejection of hepatic metastasis, we injected pCMV-IL-12 or pCMV into mice that had been intra-splenically injected with CT-26 cells 2 days earlier. Serum IFNγ levels of Rag2 KO mice were about 4 times higher than those of wild-type mice (Fig. 4b). pCMV-IL-12 completely suppressed hepatic metastasis in Rag2 KO mice (Fig. 4c).

Adoptive transfer of wild-type NK cells into GKO mice restored the anti-tumor effects of IL-12

Since NK cells were sufficient for producing IL-12-induced anti-tumor effects, we postulated that their production of IFNγ may play an important role in these effects. To test this, we performed adoptive transfer experiments with GKO mice. First, whole mononuclear cells isolated from the spleens of wild-type mice (2.0×10^8 cells) were adoptively transferred to GKO mice 1 day before plasmid injection. pCMV-IL-12 injection increased Yac1 lytic activity of hepatic mononuclear cells in the adoptively transferred group, but not in the untreated group (Fig. 5a). pCMV-IL-12 induced significant increase in serum IFNγ levels 4 days after plasmid injection in the adoptive transferred group, but not in the other groups (Fig. 5b). The

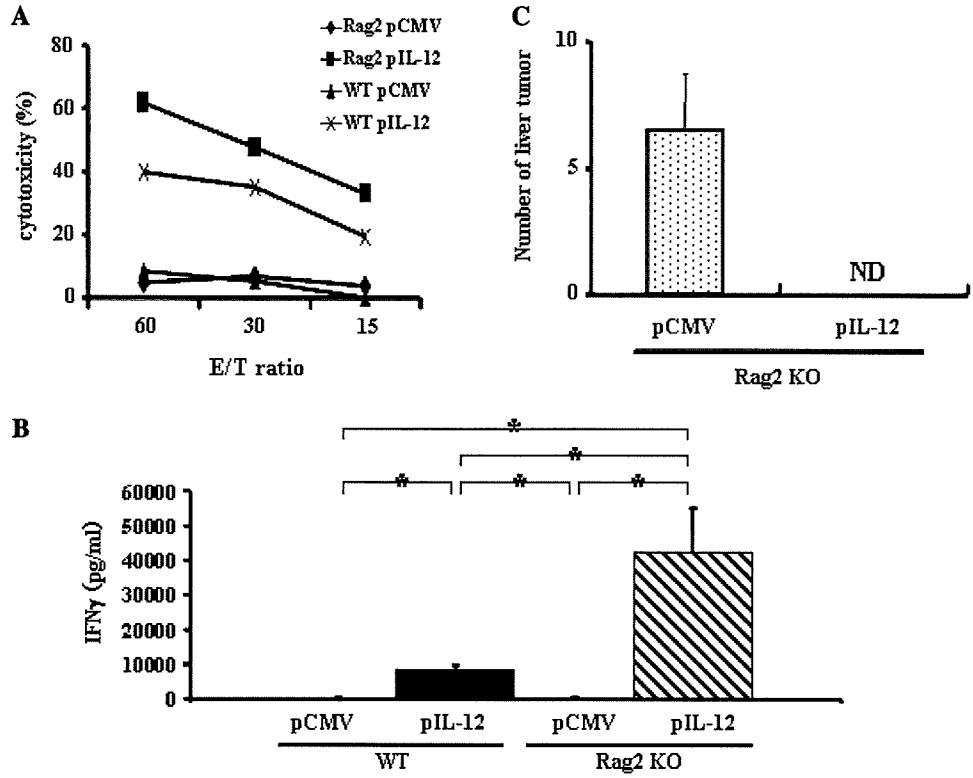

Fig. 4 Anti-tumor effects of IL-12 in Rag2 KO mice. Serum IFNγ levels and NK-cell activation. Wild-type or Rag2 KO mice were hydrodynamically injected with either pCMV-IL-12 or pCMV and killed at 4 days. **a** Yac1 lytic ability of hepatic mononuclear cells was determined by Cr releasing assay as the indicated effector and target ratios (E/T ratio). Experiments were done 2 times and representative data are shown. **b** The levels of serum IFNγ were determined by ELISA. Data are expressed as mean and SD ($n = 7$/group). *$p < 0.0001$. **c** Anti-metastatic effect. Rag2 KO mice were intrasplenically injected with CT-26 cells and, 2 days later, hydrodynamically injected with either pCMV-IL-12 or pCMV. Fourteen days after plasmid injection, mice were killed to examine tumor development in the liver. The numbers of hepatic tumors in each group are expressed as mean and SD ($n = 7$/group). *ND* not detectable

anti-metastatic effect of IL-12 was restored in GKO mice when whole mononuclear cells from wild-type mice were adoptively transferred (Fig. 5c).

To evaluate the contribution of IFNγ production from each subset of mononuclear cells to the anti-metastatic effect of IL-12, we adoptively transferred the same number of whole mononuclear cells, NK cells or non-NK cells from wild-type mice (4.0×10^6 cells) 1 day before pCMV-IL-12 injection and analyzed liver tumor formation. Only in the NK-cell-transferred group, pCMV-IL-12 injection induced NK cytolytic ability in the liver and IFNγ elevation in serum 4 days after plasmid injection, but not in the other groups (Fig. 5d, e). No liver tumor formed in the NK-cell-transferred group. In contrast, livers in other groups had massive tumors, and the liver weights were significantly heavier than those in the NK-cell-transferred group (Fig. 5f). These results clearly demonstrated the strong impact of IFNγ produced from NK cells on IL-12-induced anti-tumor effects compared with that from non-NK cells.

Anti-tumor effects of IL-12 deteriorated slightly in mice depleted of NK cells

To examine the involvement of NK cells in the tumor deletion by IL-12 therapy, we induced depletion of NK cells by repeatedly injecting anti-asialoGM1 antibody. The cytolytic ability of NK cells was completely abolished in the anti-asialoGM1 antibody-injected group (Fig. 6a). Serum IFNγ induction by IL-12 in the NK depletion group was about half of that in the control immunoglobulin injected group (Fig. 6b). Unexpectedly, pCMV-IL-12 injection inhibited macroscopic liver metastasis of CT-26 cells in NK cell-depleted mice (Fig. 6c). However, a number of microscopic tumor regions were observed after IL-12 therapy in NK cell-depleted mice but not in control IgG-injected mice (Fig. 6d). This finding indicated that NK cells are required for a full-blown IL-12 anti-tumor effect, but IL-12's anti-tumor effect was still observed even if the NK cells were knocked down. To examine the underlying mechanisms of anti-tumor effect in NK cell-depleted mice,